

**A proposed mechanism for non-carious cervical lesions, root resorption and
abutment screw loosening**

Running title: NCCL, root resorption and abutment screw loosening

Thomas R. Katona (Corresponding author)
ORCID: 0000-0001-9949-7237

Purdue School of Engineering and Technology
Department of Mechanical Engineering and Energy

Department of Orthodontics and Oral Facial Genetics
Indiana University School of Dentistry
1121 W. Michigan St., Indianapolis, IN 46202, USA
tkatona@iu.edu

George J. Eckert
ORCID: 0000-0001-7798-7155
Department of Biostatistics and Health Data Science
Indiana University School of Medicine, Indianapolis, USA
geckert@iu.edu

Keywords: Occlusion, Periodontal ligament, Non-carious cervical lesions, Root resorption,
Abutment screw, Bruxism

Conflict of interest: The authors have no conflicts of interest to declare.

A proposed mechanism for non-carious cervical lesions, root resorption and abutment screw loosening

ABSTRACT

Objectives

The purpose of this paper is to present a mechanism for the shared etiologies of non-carious cervical lesions (NCCLs), orthodontics-associated root resorption and implant abutment screw loosening. These are persistent clinical problems with equivocal etiologies.

Methods

A matched pair of 1st molar denture teeth was set into occlusion within a testing apparatus. The weighted maxillary assembly, guided by slides, was cyclically lowered onto, and raised from, the mandibular tooth. The forces and moments on the mandibular tooth were continuously recorded by a load cell. The maxillary crown was rigidly fixed (ankylosed or implant supported). The mandibular tooth was rigidly fixed or supported by a PDL analogue. For statistics, 21 occlusal relationships were tested.

Results

The measurements confirmed earlier non- and counter-intuitive results. The directly relevant data were that the measured loads on the tooth, during the span of an *individual* chomp, are characterized by a wide range of magnitudes and directions. Moreover, these load profiles change with rigid vs. PDL support ($p = 0.001$), occlusal relationship ($p < 0.001$) and occlusion vs. disclusion ($p = 0.002$).

Conclusion

The demonstrated transient loads within the span of a single chomp produce complex mechanical environments. Thus, it is proposed that NCCLs, orthodontic root resorption and abutment screw loosening result from load component *combinations*, not from solitary occlusion forces as typically applied in experimental and numerical investigations. In principle, the loading combination concept applies to all phenomena that involve occlusal contacts, including occlusal trauma, implant loading, jaw fracture repairs, etc.

The mechanics of non-carious cervical lesions, root resorption and abutment screw loosening – a proposed mechanism

INTRODUCTION

In the occlusion mechanics-related literature, the focus is typically on force magnitudes. But force directions are no less important in the governing engineering principles and the associated physiology. And, consideration of the attendant moments is usually absent. Furthermore, it has been demonstrated^{1,2} that occlusal contact forces (and therefore, the moments they generate) continuously change in magnitude and/or direction *during* the course of a single chomp (a complete bite cycle). These transient load (force and moment) magnitudes and directions throughout the 3 phases of a chomp (occlusion – clench – disclusion) have clinical and experimental ramifications. (In this context, “occlusion” refers to the period between the initial tooth contact and full bite force. “Clenching” is the period of full bite force application, and “disclusion” is the interval between the release of full-force and complete separation.)

The prevailing notion that the forces experienced by an occluding tooth can be considered, or modelled, as unidirectional and/or of constant magnitude, may be the reason for some enduring “mysteries.” Three such examples are the elusive etiologies of non-carious cervical lesions (NCCLs),³⁻⁸ orthodontic root resorption⁹⁻¹¹ and implant abutment screw loosening.¹²⁻¹⁴ It is proposed that these clinical complications can be attributed to the *transient* mechanical environments that are associated with occlusal surface contacts.

Thus, the purpose of this study is to present mechanisms, based on the transient functional loads experienced by the dentition during individual chomps, for the etiologies of NCCLs, root resorption and abutment screw loosening.

Materials and Methods

Brief description

The data for this project were derived from a previously published study¹ in which a weighted maxillary molar denture tooth was cyclically lowered onto, and raised from, the matching mandibular tooth. The loads (forces and moments) acting on the mandibular tooth were continuously measured by the load cell that supported the tooth. Tests were conducted with 21 precise shifts of the mandibular assembly, each with rigid (control) and PDL analogue mandibular tooth attachment.

PDL analogue

The PDL analogue¹⁵ consisted of a 50:50 mixture of gasket sealant No. 2 (GS 30515, supplanted by Loctite 198819) and RTV 587 silicone (RTV 30560, supplanted by Loctite 270642), both by Henkel Corp, Düsseldorf, Germany.

Testing apparatus

The testing apparatus, **Figure 1A**, contained a pair of vertical precision slides (Mini-Guide, Double Carriage, Model #SEBS 9BUU2-275, Nippon Bearing Co, Ojiya, Japan) to guide the maxillary tooth assembly that was weighted down to ~19 N. A mechanical testing machine (MTS Bionix 858, MTS Corporation, Minneapolis, MN, USA) was programmed to raise and lower the maxillary assembly.

Force (F_x , F_y and F_z) and moment (M_x , M_y and M_z) components acting on the mandibular tooth (**Figure 1A, B**) were measured by a load cell (Gamma transducer SI-65-5, ATI Industrial Automation, Apex, NC, USA) at $0-65 \pm 0.0125$ (N) and $0-5000 \pm 0.9$ (N-mm), respectively. The load cell measurements were recorded (at 100 Hz) by a (generic) laptop computer via NI-DAQmx software (National Instruments Corporation, Austin, TX, USA).

Specimen preparation

First, the denture teeth were mounted into their respective holders. Both holders, 10 x 10 x 28 mm overall, precision-machined aluminum bars, had large cylindrical holes in one end to receive the denture teeth and a threaded mounting hole in the other. However, the mandibular part is an assembly of a “tooth” with a conical root (30° and 8 mm diameter at the CEJ) in a matching socket (**Figure 1B, C**).

Maxillary and mandibular Portrait IPN 33° (Dentsply, York, PA, USA) right first molar denture teeth were trimmed to fit into the cylindrical holes of the holders, the maxillary tooth was fixed in position with generic orthodontic resin and mounted onto the testing apparatus. The 2 parts of the mandibular holder were taped together with (generic) cellophane tape, screwed to its holding plate, and placed on the instrument’s table. The mandibular denture tooth was seated into its holder that was $\sim\frac{3}{4}$ filled with slightly cured orthodontic resin, then, under gentle occlusal contact, the lower assembly was slid into a Class I relationship and allowed to cure in position. Then, the tape was removed.

And finally, the PDL analogue was painted onto the root and socket surfaces with micro-brushes (Kerr Applicators, Part No. 24680, Kerr Corporation, Orange, CA, USA). The root and socket were loosely assembled, the alignment jig (**Figure 1C**) was tightened against the “bone” with the 2 lower setscrews, the top setscrew was slightly tightened against the “crown”, two 1.0 mm spacers (0.04 inch diameter orthodontic wires) were inserted between the “crown” and “bone,” and as the crown was pushed down against the wires, the top setscrew was fully tightened. With the wires removed, the overflow was cleaned off and the 0.3 mm analogue layer cured for 3 days.

Testing set-up

The upper portion was rested on the complete lower assembly that consisted of the mandibular specimen, with the tightened alignment jig, mounted on the load cell. The lower part was moved about slightly until the maxillary tooth “fell” into the centric Class I position. At this point, the lower assembly was clamped in-place. 0.20 mm thick gages (Feeler Stock No. 667-8, L. S. Starrett Co., Athol, MA, USA) were placed between both sides of a generic carpenter square and the rectangular base of the load cell. The carpenter square was then clamped to the table for the duration of the experiment. The 21 precisely controlled shifts (**Figure 1D**) in the occlusal relationship were obtained by replacing the shims in 0.05 mm thickness increments.

Testing

As indicated by a slight slack in the supporting chain, the full bite force ($F_z \cong 19$ N) was applied manually by lowering the MTS machine’s hydraulic actuator. This was set as the zero-position of the actuator. Then, ramp-displacement control (0.2 Hz at 8.0 mm amplitude) was applied for a 10-chomp cycle while the loads on the mandibular tooth were measured at 100 Hz by the load cell. At each of the 21 occlusal relationships (shaded positions in **Figure 1D**), the 10-chomp cycle was run twice – once with the jig clamped in position (**Figure 1C**, without the wire spacers) to achieve rigid attachment (control), and with the 3 setscrews fully loosened for PDL support.

Sample size and statistical analysis

Based on previous studies, the coefficient of variation was estimated to be 1.6. With a sample size of $n = 21$ occlusion positions, the study had 80% power to detect a 3x difference in occlusal loads between groups, assuming a 5% significance level for each test. Peak values of F_x , F_y , $F_{lateral}$, M_x , M_y and M_z were analyzed, **Table 1**. The data were not normally distributed, so all comparisons were performed using nonparametric Friedman’s tests.

RESULTS

Analysis of $F_{lateral}$ (**Figure 1B**) from the recent model¹ that forms the basis of this paper, showed that there are statistically significant differences associated with rigid vs. PDL support ($p = 0.001$), occlusal relationships ($p < 0.001$) and occlusion vs. disclusion ($p < 0.001$ in F_x , F_y , M_x , M_y and $p = 0.024$ in M_z), **Table 1**.

To illustrate results, measurements for configuration 2520 (mandibular assembly shifted 0.05 mm lingually from centric) are presented in **Figures 2** and **3** for the 5th chomp. (Chomp-to-chomp differences are sufficiently small for this purpose to allow a single chomp to serve as the exemplar.) The circles and squares indicate the data points for $F_z = 15$ N in occlusion ($F_z = 0 \dots \rightarrow \dots 15 \dots \rightarrow \dots \sim 19$ N) and then disclusion ($F_z = \sim 19 \dots \rightarrow \dots 15 \dots \rightarrow \dots 0$ N), respectively. With F_x plotted against F_y , **Figure 2**, the dashed arrows between the origin and the \circ and \square symbols represent the in-occlusal-plane $\mathbf{F}_{lateral}$ force vectors that act on the mandibular tooth when $F_z = 15$ N. The same data, but with F_x and F_y plotted against the bite force, F_z , are

shown in **Figure 3A, C**, respectively, for the PDL and rigid attachments. Similarly, the moment components (M_x , M_y , $10M_z$) are plotted in **B** and **D**.

In **Figure 4A - D**, each cluster of 5 points, the 2 force components [F_x (●) and F_y (■)] and the 3 moment components [M_x (○), M_y (□) and $10M_z$ (Δ)], represents the load profile on the mandibular tooth during the 5th chomp when the bite force (F_z) is 15 N. Each of the 4 clusters in each panel is a different occlusal configuration. The results for the 4 occlusal relationships that are closest (0.05 mm) to centric (1520, 2015, 2025, and 2520) are in **A** (PDL) and **C** (rigid), and similarly, **B** and **D** show the data for the 4 occlusal positions (0000, 0040, 4000 and 4040) that are furthest (0.283 mm) from centric. (In this figure, for simplicity, the force and moment components are the averaged occluding and discluding values.)

DISCUSSION

Forces and moments are vector quantities as they are characterized by magnitude and direction. To define a *force* vector, its point-of-application (or line-of-action) must be also specified. In typical numerical and bench-top studies involving occlusal contact forces, the force vector (often cyclic in experiments) is applied directly to the crown at a specific location and direction¹⁶⁻¹⁹ or, separately, at multiple locations and/or directions.^{17,20-23} But, our measurements demonstrate that cusped occlusal surface contacts produce wide ranges of force magnitudes and directions *during individual* chomps, **Figures 2** and **3**,^{1,24,25} because the loads are generated by multiple simultaneous cusp-tip/incline – cusp-tip/incline contacts that change as the bite force is applied (occlusion) or removed (disclusion), as well as during the intervening clench period if a viscoelastic PDL analogue is present.¹

Indeed, an FEA study has shown that tooth antagonists (*i.e.*, multiple cusp contacts) produce different levels of stresses within implant-supporting bone than those produced by a specified direct load.²⁶ Furthermore, the same study showed that differences in antagonists create different bone stresses. As the stresses are produced by the forces of occlusal contacts, our results are in concordance with their findings. The lab results also demonstrate, as emphasized above, that the systems of loads generated by crown antagonists (*i.e.*, cusped occlusal surfaces) change significantly *within* the span of a single chomp, **Figures 2** and **3**.

Thus, the premise for the proposed shared mechanism for the etiologies of NCCLs, root resorption and abutment screw loosening are these complex transient mechanical environments that are produced by multiple simultaneous occlusal surface cusp contacts. This is in contrast to the unchanging mechanical environments associated with the traditionally prescribed experimental and numerical singular occlusal contact forces.

In this experiment, the Rigid/PDL combination (maxillary implant opposing a natural mandibular tooth) is applicable to mandibular NCCLs and root resorption. The Rigid/Rigid (opposing implants) data are relevant to the mandibular abutment screw problem. (Rigid/Rigid would also apply to NCCLs on an ankylosed tooth opposing an implant, or another ankylosed tooth, but we have not found relevant literature about NCCLs on ankylosed teeth.)

It has previously been shown (**Figures 2 - 4**) that Rigid/Rigid generates higher forces than Rigid/PDL.¹ Thus, the inclination is to conclude that an abutment screw is more likely to loosen if it opposes another implant rather than a natural tooth. And, by extrapolation, NCCLs and root resorption should be more prevalent and severe in teeth that oppose an implant than in teeth that oppose a natural tooth. These conclusions may-or-may-not be correct (we found no relevant literature), but for the proposed mechanism, it makes no difference as high forces are not necessarily the blamed culprits.

As noted above, the suggested mechanism for NCCLs, root resorption and the loosening of abutment screws is based on the variety of loads experienced by teeth in the course of a single chomp, **Figures 2 - 4**. In **Figures 4A - D**, $F_z = 15$ N, and as shown in **Figures 4A, C**, the load profiles change even with small (0.05 mm) changes in the occlusal relationship. The results are also affected by human saliva, the type of artificial saliva, the type of occlusal surface material (denture, ceramic, stainless steel), and cusp angulation.^{1,2,24,25}

As an example, compare the results highlighted, dashed boxes, in **Figure 4C**. The load profile experienced by the tooth in configuration 1520 consists of an F_x (●) ≈ 0 , a relatively high F_y (■) in the negative (distal) direction, an M_x (○) in the negative (buccal) direction, ~ 0 M_y (□), and a small M_z (△) in the negative direction. With the same 15 N bite force (F_z), the load profile on configuration 2520 (which is 0.1 mm lingual to the 1520) is entirely different from that of 1520, most notably, irrespective of magnitude, every load component is in the opposite direction.

Consider opening a child-proof medicine bottle, **Figure 5A**. As the cap is being turned, it has to be pushed-down. In the nomenclature of this paper, a $-M_z$ and a downward F_z must be applied concurrently, **Figure 5B**. If applied separately, the cap will not open. The presented hypothesis is that, analogous to the bottle opening, NCCLs and root resorption develop and/or progress, and abutment screws loosen, when the structures experience some specific simultaneous *combination(s)* of 2, or more, load components, **Figure 5**. It is very unlikely that it would be the same combination for the 3 clinical problems. And, it would be coincidental if a typical experimental/numerical loading scheme would replicate an efficacious mechanical environment for producing any of the 3 clinical problems.

For illustrative purposes, suppose that loosening a mandibular abutment screw required the same mechanical environment as opening the bottle cap, *i.e.*, simultaneous downward F_z and $-M_z$, **Figure 5B**. The model to consider is Rigid/Rigid, **Figure 4C** and **D**. In these figures, the 15 N F_z is downward, which meets the F_z requirement. In all instances, M_z is relatively small, but configurations 1520, 2015, 0000 and 4000 meet the $M_z < 0$ condition. Thus, according to the proposed hypothesis, of the 8 configurations, these 4 have the *potential* to loosen the screw. (The other 4, with $M_z > 0$, would tend to tighten the screw.)

The abilities of the 4 load systems to loosen the screw are qualified as “potential” because there are other factors to consider. For one, the magnitude ranges of the force and moment components must be taken into account. In these examples, the 15 N F_z may be sufficient, but the M_z s may be too small. Furthermore, it must be recognized that the other load components (F_x , F_y , M_x and M_y) are relatively high, and it is unclear if in the abutment assembly they would hinder, or assist, the loosening process. To open the medicine bottle, they would be hindrances.

Thus, the absence of some load components may be just as important as the presence of the necessary ones.

The proposed mechanism is, in fact, not a new concept to dentistry. In forceps extractions, the tooth is luxated back-and-forth, but at the same time, it must be intruded. That is because the root is weak in tension but strong in compression, so it tends to break on the tension side when bent during luxation. The simultaneous intrusive force increases the compression in the root, which is acceptable, but it also decreases the tension, which is necessary. Schematically, in **Figure 5B**, the extraction loading would be shown as an intrusive F_z with a $\pm M_y$. Similarly, the tightening/loosening of an ordinary screw requires a push (F_z) on the screwdriver handle to keep the blade engaged in the slot, plus a simultaneous $\pm M_z$ to turn the screw.

Although controversial, orthodontic tooth movement has been linked to root resorption.^{10,11,27} In the proposed mechanism of root resorption, orthodontic forces (which are relatively small compared to occlusal forces) have two critical roles. One is that they stimulate the clastic activity that is necessary for root movement through bone and the resorption of damaged root surfaces. The second role is that they move the tooth, thereby altering its occlusion. Thus, during the course of treatment, a tooth could be shifted, for example, 0.1 mm buccally from position 2520 to position 1520 (dashed boxes in **Figure 4C**). That could change the mechanical environment from one that is, for the sake of argument, benign, to one that is root-damaging. Once compromised, the damaged root surface is resorbed. Thus, orthodontic forces are intimately, but indirectly, involved in root resorption.

Likewise, it is proposed that the suggested root resorption mechanism also applies to the formation and progression of occlusion-related NCCLs, which are, after all, damage at a different level on the root. A difference is that in the root resorption scenario, odontoclasts eliminate the weakened dentin, but it is likely that a toothbrush has that role with the abfraction-compromised NCCL root surfaces.

The proposed mechanism provides a unified alternative to traditional approaches that have been unable to adequately explicate NCCLs, orthodontic root resorption and abutment screw loosening. The key commonality is the concept that it is some *combination(s)* of force and moment components (**Figures 4A - D**) that act on the tooth to create the clinical issues. The most efficacious problematic load combinations are more likely to be realized during the complex multiple contact interactions of cusped occlusal surfaces, as in this experiment, than in typical models with prescribed simple loading conditions. Compare the elaborate loading profiles of cusped surface occlusal contacts, **Figures 4A - D**, with those of pure intrusive (F_z) or lingually (F_x) directed forces, **Figure 4E**, common loading conditions in numerical and laboratory models. In terms of the bottle cap analogy, **Figure 5**, traditional studies do not apply combinations of F_z and M_z . (In some instances, inadvertent experimental force misalignments may serendipitously produce different results.)

Earlier, it was stated that, for simplicity, in **Figures 4A - D**, the displayed force and moment component magnitudes consist of the averages of significantly different (**Table 1**) occlusion and disclusion measurements. Furthermore, the presented data are specific to a 15 N bite force (F_z), but as evident in **Figure 3**, the force and moment components change with the magnitude of F_z .

Thus, for both reasons, the tooth experiences a far larger number of load combinations than depicted in **Figure 4**.

Bruxism adds a layer of complexity as it increases the variability in the bite force magnitude, and perhaps more importantly, direction. A bruxing bite force is not purely vertical, as it is in this experiment, so in addition to F_z , bruxing also applies an F_x and/or an F_y . (These are in addition to the F_x and F_y produced by the occlusal contacts.) Thus the role of bruxism, if any, in NCCLs, orthodontic root resorption and abutment screw loosening, etc., may be attributed to the large number of load combinations (**Figure 4**) that it produces, thereby enhancing the possibility of a detrimental combination. Thus, bruxism, per se, would not be the cause of these clinical issues, rather it may be bruxism in a specific direction(s) that is related to the unique occlusal anatomies of the contacting surfaces.

It should be noted that, conceptually, the proposed mechanism applies to a myriad of other dental problems in which occlusal contact forces play a role, including implant loading, occlusal trauma, TMD, wear facets, bruxing, clenching, dental bite pain, crown and root fractures, restorative longevity and jaw fracture repairs.

References

1. deMoya AV, Schmidt ER, Eckert GJ, Katona TR. The effects of a periodontal ligament analogue on occlusal contact forces. *J Oral Rehabil.* 2021.
2. McCrea ES, Katona TR, Eckert GJ. The effects of salivas on occlusal forces. *J Oral Rehabil.* 2015;42(5):348-354.
3. Duangthip D, Man A, Poon PH, Lo ECM, Chu CH. Occlusal stress is involved in the formation of non-cariou cervical lesions. A systematic review of abfraction. *Am J Dent.* 2017;30(4):212-220.
4. Alvarez-Arenal A, Alvarez-Menendez L, Gonzalez-Gonzalez I, Alvarez-Riesgo JA, Brizuela-Velasco A, deLlanos-Lanchares H. Non-cariou cervical lesions and risk factors: A case-control study. *J Oral Rehabil.* 2019;46(1):65-75.
5. Hur B, Kim HC, Park JK, Versluis A. Characteristics of non-cariou cervical lesions--an ex vivo study using micro computed tomography. *J Oral Rehabil.* 2011;38(6):469-474.
6. Senna P, Del Bel Cury A, Rosing C. Non-cariou cervical lesions and occlusion: a systematic review of clinical studies. *J Oral Rehabil.* 2012;39(6):450-462.
7. Silva AG, Martins CC, Zina LG, et al. The association between occlusal factors and noncariou cervical lesions: a systematic review. *J Dent.* 2013;41(1):9-16.
8. Igarashi Y, Yoshida S, Kanazawa E. The prevalence and morphological types of non-cariou cervical lesions (NCCL) in a contemporary sample of people. *Odontology.* 2017;105(4):443-452.
9. Elhaddaoui R, Qoraich HS, Bahije L, Zaoui F. Orthodontic aligners and root resorption: A systematic review. *Int Orthod.* 2017;15(1):1-12.
10. Roscoe MG, Meira JB, Cattaneo PM. Association of orthodontic force system and root resorption: A systematic review. *Am J Orthod Dentofacial Orthop.* 2015;147(5):610-626.
11. Currell SD, Liaw A, Blackmore Grant PD, Esterman A, Nimmo A. Orthodontic mechanotherapies and their influence on external root resorption: A systematic review. *Am J Orthod Dentofacial Orthop.* 2019;155(3):313-329.
12. Huang Y, Wang J. Mechanism of and factors associated with the loosening of the implant abutment screw: A review. *J Esthet Restor Dent.* 2019;31(4):338-345.
13. Katsavochristou A, Koumoulis D. Incidence of abutment screw failure of single or splinted implant prostheses: A review and update on current clinical status. *J Oral Rehabil.* 2019;46(8):776-786.
14. Armentia M, Abasolo M, Coria I, Bouzid A-H. On the Use of a Simplified Slip Limit Equation to Predict Screw Self-Loosening of Dental Implants Subjected to External Cycling Loading. *Applied Sciences.* 2020;10(19):6748.
15. Xia Z, Chen J. Biomechanical validation of an artificial tooth-periodontal ligament-bone complex for in vitro orthodontic load measurement. *Angle Orthod.* 2013;83(3):410-417.
16. Machado AC, Soares CJ, Reis BR, Bicalho AA, Raposo L, Soares PV. Stress-strain analysis of premolars with non-cariou cervical lesions: Influence of restorative material, loading direction and mechanical fatigue. *Oper Dent.* 2017;42(3):253-265.
17. Guimaraes JC, Guimaraes Soella G, Brandao Durand L, et al. Stress amplifications in dental non-cariou cervical lesions. *J Biomech.* 2014;47(2):410-416.
18. Zeola LF, Pereira FA, Machado AC, et al. Effects of non-cariou cervical lesion size, occlusal loading and restoration on biomechanical behaviour of premolar teeth. *Aust Dent J.* 2016;61(4):408-417.

19. Chang HC, Li HY, Chen YN, Chang CH, Wang CH. Mechanical analysis of a dental implant system under 3 contact conditions and with 2 mechanical factors. *J Prosthet Dent.* 2019;122(4):376-382.
20. Du JK, Wu JH, Chen PH, Ho PS, Chen KK. Influence of cavity depth and restoration of non-carious cervical root lesions on strain distribution from various loading sites. *BMC Oral Health.* 2020;20(1):98.
21. Tanaka M, Naito T, Yokota M, Kohno M. Finite element analysis of the possible mechanism of cervical lesion formation by occlusal force. *J Oral Rehabil.* 2003;30(1):60-67.
22. Yang S-M, Chung H-J. Three-dimensional finite element analysis of a mandibular premolar with reduced periodontal support under a non-axial load. *Oral Biol Res.* 2019;43:313-326.
23. Benazzi S, Grosse IR, Gruppioni G, Weber GW, Kullmer O. Comparison of occlusal loading conditions in a lower second premolar using three-dimensional finite element analysis. *Clin Oral Investig.* 2014;18(2):369-375.
24. Beninati CJ, Katona TR. The combined effects of salivas and occlusal indicators on occlusal contact forces. *J Oral Rehabil.* 2019;46(5):468-474.
25. Mitchem JA, Katona TR, Moser EAS. Does the presence of an occlusal indicator product affect the contact forces between full dentitions? *J Oral Rehabil.* 2017;44(10):791-799.
26. Rand A, Stiesch M, Eisenburger M, Greuling A. The effect of direct and indirect force transmission on peri-implant bone stress - a contact finite element analysis. *Comput Methods Biomech Biomed Engin.* 2017;20(10):1132-1139.
27. Vicilli RF, Katona TR, Chen J, Hartsfield JK, Jr., Roberts WE. Three-dimensional mechanical environment of orthodontic tooth movement and root resorption. *Am J Orthod Dentofacial Orthop.* 2008;133(6):791 e711-726.

FIGURE LEGENDS

FIGURE 1 The testing apparatus. (A) Picture. (B) While the bite force (F_z) acts on the crown, the load cell measures the reaction force (F_x and F_y) and moment (M_x , M_y and M_z) components that support the tooth. The magnitude and direction of the in-occlusal-plane force, $\mathbf{F}_{\text{lateral}}$, acting on the tooth are given by:

$$F_{\text{lateral}} = \text{SQRT}(F_x^2 + F_y^2) \quad \text{and} \quad \theta = \text{ATAN}(F_y/F_x),$$

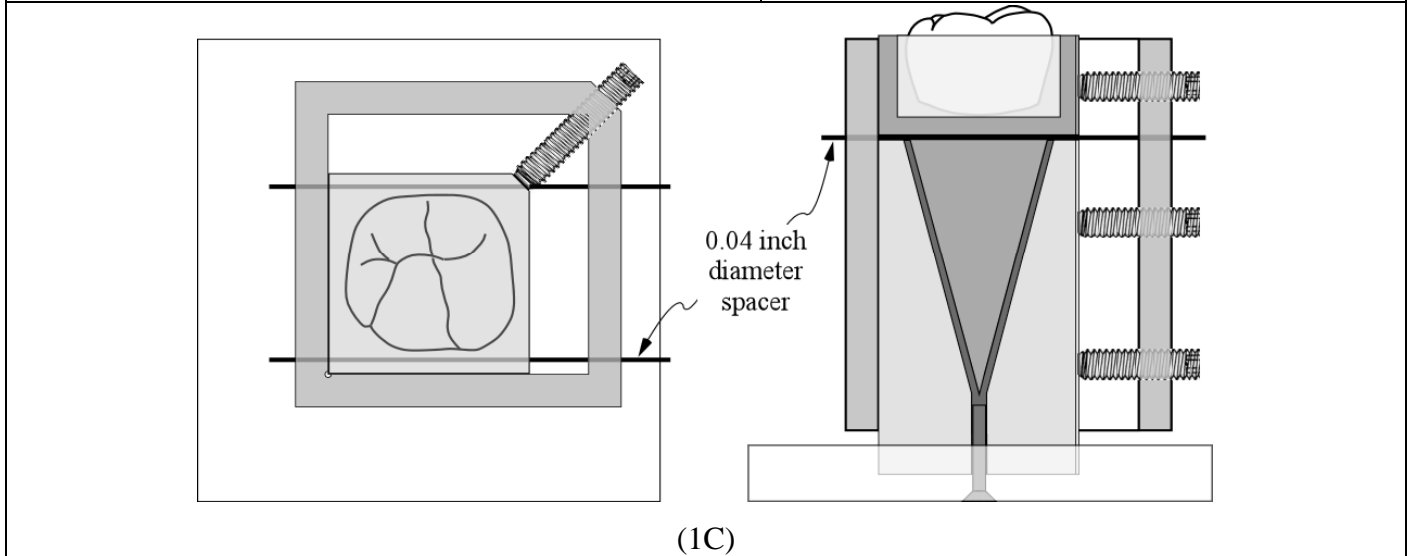
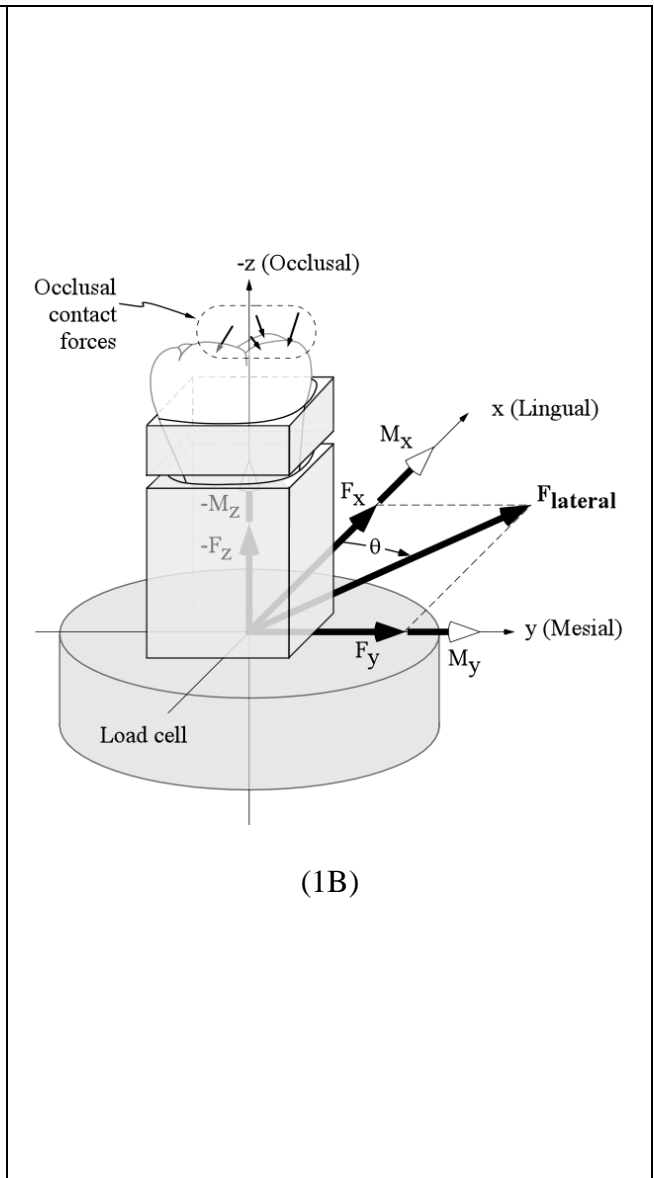
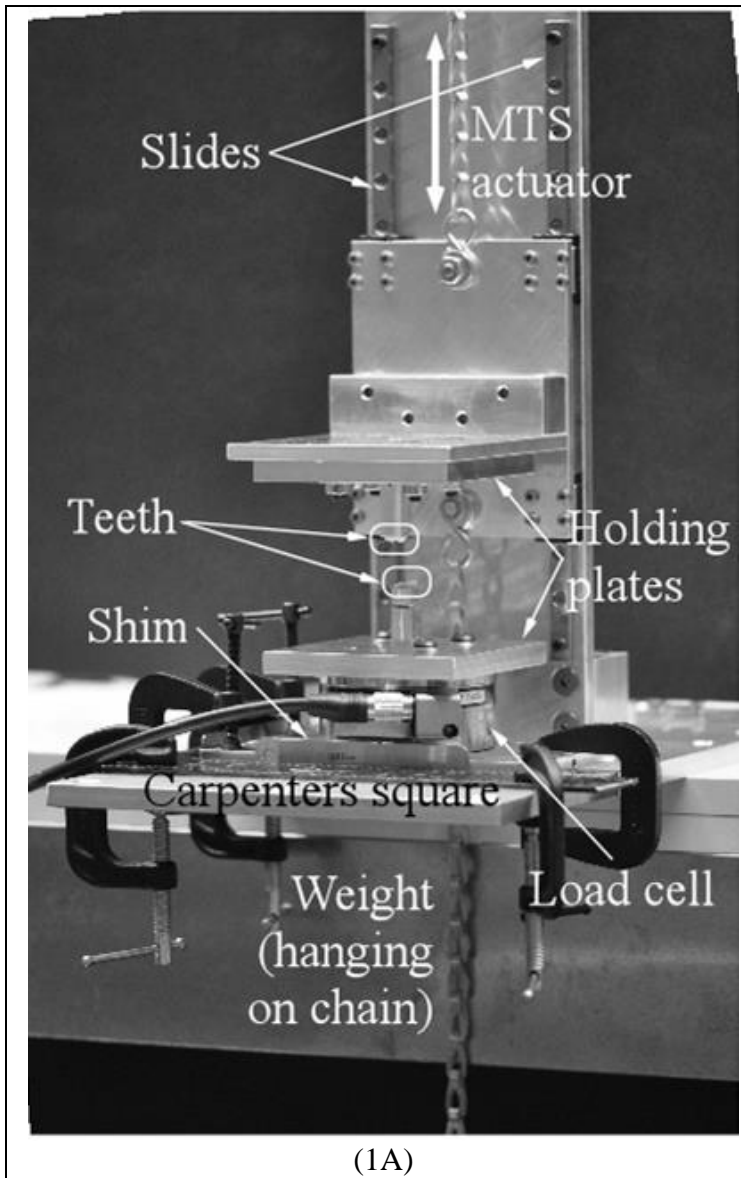
and the directions of the moment components are according to the right-hand-rule. (C) Schematics of the PDL polymerization alignment jig. Once cured, the wires were removed. Thereafter, PDL and rigid support were achieved, respectively, by fully loosening or tightening the 3 setscrews. (D) The 0.05 mm grid on the left shows the 21 tested positions (shaded) of the mandibular tooth and the 4 closest and 4 furthest positions from centric, bolded. In the notation $xxyy$, xx refers to the x (lingual)-coordinates (in $1/100^{\text{th}}$ of a mm) of the position. Similarly for yy . The shim arrangements for centric (2020) and 2 other positions are illustrated on the right

FIGURE 2 PDL and rigid data (F_x vs. F_y) for the 5th chomp of configuration 2520. The 4 dashed force vector arrows graphically illustrate the $\mathbf{F}_{\text{lateral}}$ that act on the crown during occlusion (\circ) and disclusion (\square) when $F_z = 15$ N

FIGURE 3 F_x , F_y , M_x , M_y and M_z vs. F_z for the 5th chomp of configuration 2520 for PDL (A and B) and rigid (C and D). Note that $10 \times M_z$ is plotted. As in **Figure 2**, \circ and \square indicate occlusion and disclusion, respectively when $F_z = 15$ N

FIGURE 4 The circles, squares and triangles represent, respectively, the x -, y - and z -components of the forces (solid symbols) and moments (open symbols). In A - D, $F_z = 15$ N, which, if shown, would be represented by \blacktriangle . The M_z data (Δ) are graphed as $10 \times M_z$. (A and B) PDL in the 4 configurations closest to centric and the 4 configurations furthest from centric, respectively. Similarly, (C and D) are for the rigid attachment. (E) Examples of typical experimental loading protocols

FIGURE 5 The instruction for opening the child-proof medicine bottle is “Push down & turn”. (More precisely, it should read, “While pushing down, turn”.) Consistent with our nomenclature, it would be “While applying an F_z , apply a $-M_z$ ”



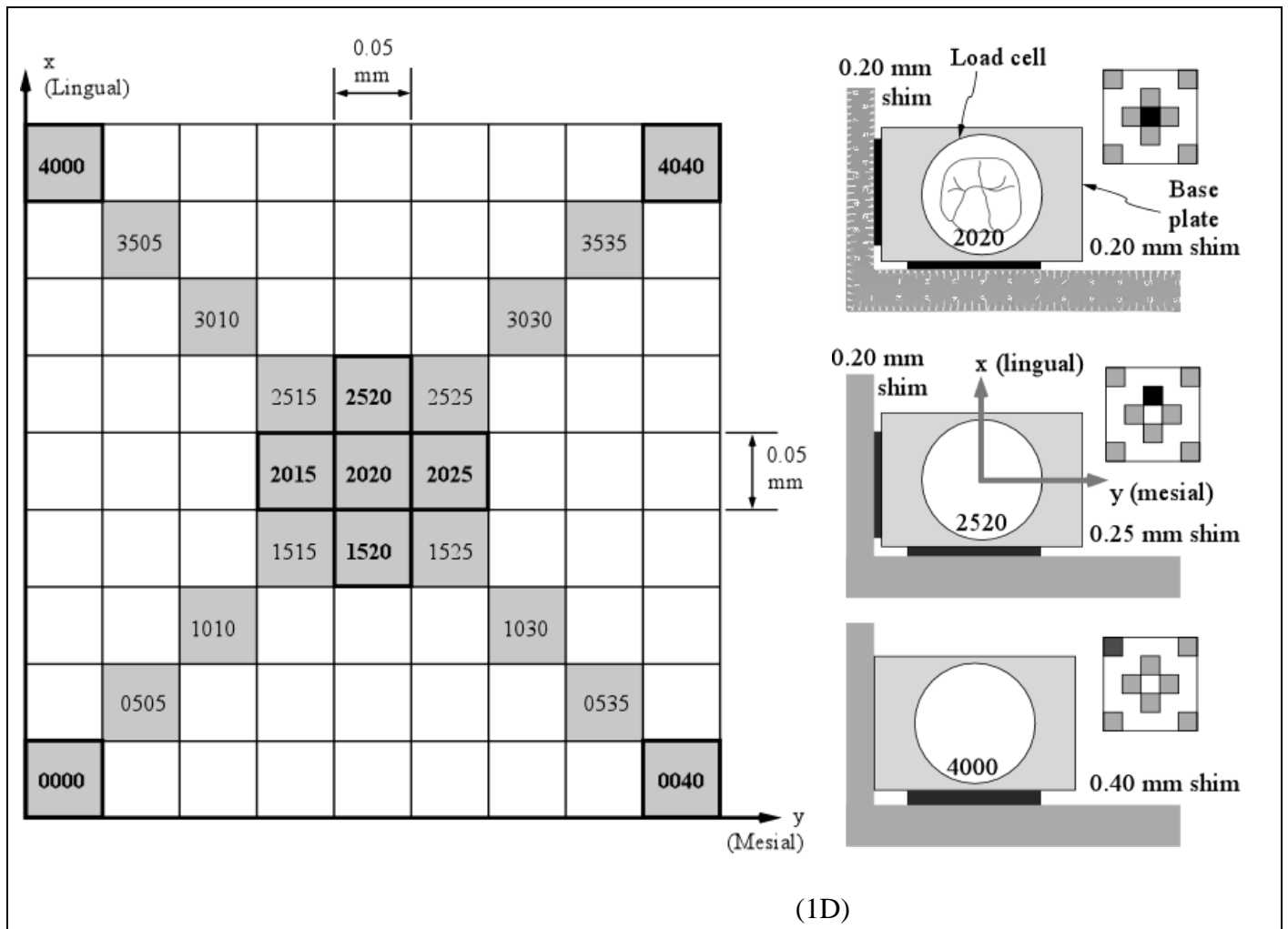


FIGURE 1 The testing apparatus. (A) Picture. (B) While the bite force (F_z) acts on the crown, the load cell measures the reaction force (F_x and F_y) and moment (M_x , M_y and M_z) components that support the tooth. The magnitude and direction of the in-occlusal-plane force, $F_{lateral}$, acting on the tooth are given by:

$$F_{lateral} = \sqrt{(F_x)^2 + (F_y)^2} \text{ and } \theta = \text{ATAN}\left(\frac{F_y}{F_x}\right),$$

and the directions of the moment components are according to the right-hand-rule. (C) Schematics of the PDL polymerization alignment jig. Once cured, the wires were removed. Thereafter, PDL and rigid support were achieved, respectively, by fully loosening or tightening the 3 setscrews. (D) The 0.05 mm grid on the left shows the 21 tested positions (shaded) of the mandibular tooth and the 4 closest and 4 furthest positions from centric, bolded. In the notation $xxyy$, xx refers to the x (lingual)-coordinates (in $1/100^{\text{th}}$ of a mm) of the position. Similarly for yy . The shim arrangements for centric (2020) and 2 other positions are illustrated on the right

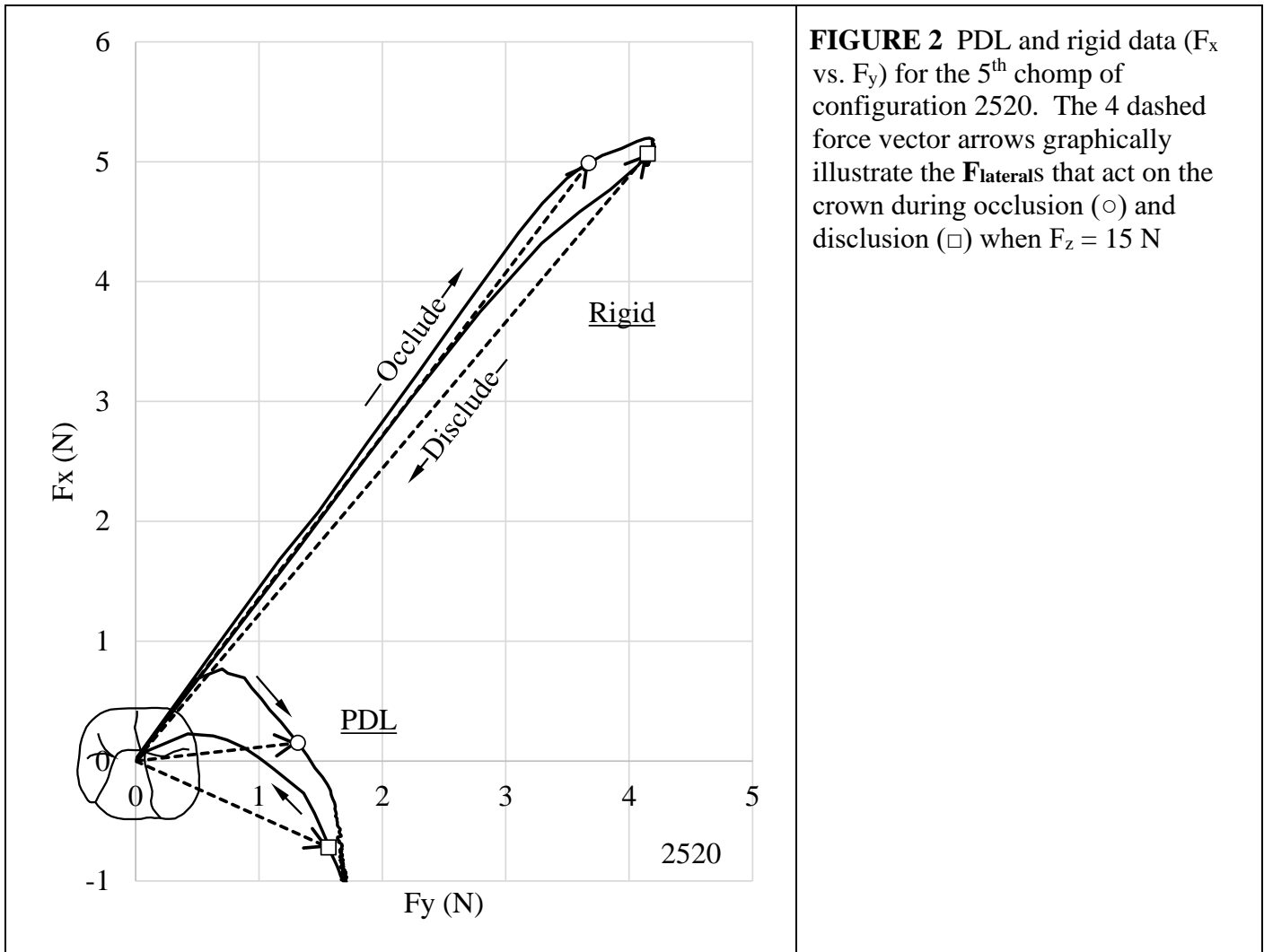


FIGURE 2 PDL and rigid data (F_x vs. F_y) for the 5th chomp of configuration 2520. The 4 dashed force vector arrows graphically illustrate the $F_{laterals}$ that act on the crown during occlusion (\circ) and disclusion (\square) when $F_z = 15$ N

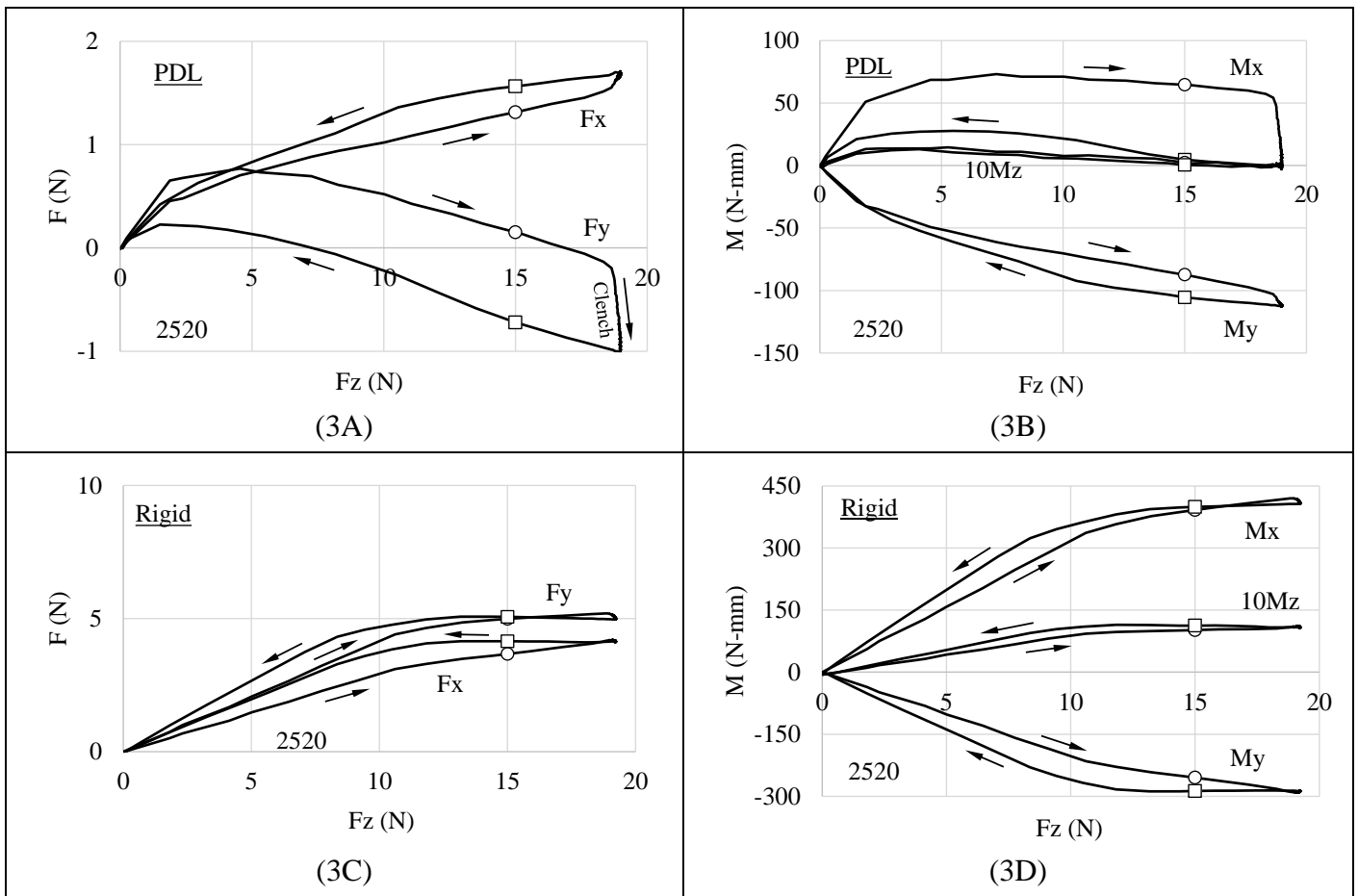


FIGURE 3 F_x , F_y , M_x , M_y and M_z vs. F_z for the 5th chomp of configuration 2520 for PDL (A and B) and rigid (C and D). Note that 10 x M_z is plotted. As in **Figure 2**, \circ and \square indicate occlusion and disclusion, respectively when $F_z = 15$ N

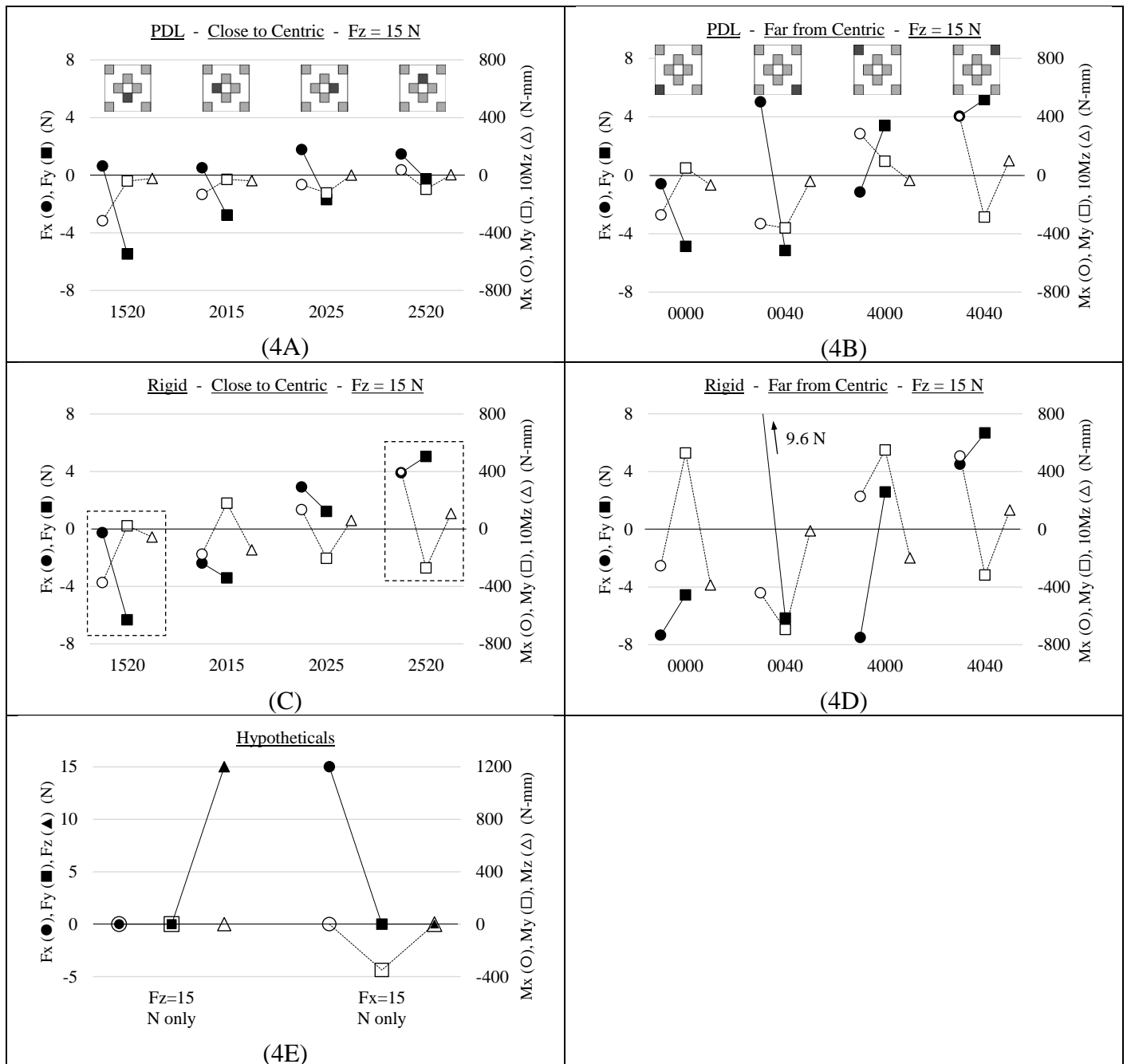


FIGURE 4 The circles, squares and triangles represent, respectively, the x-, y- and z-components of the forces (solid symbols) and moments (open symbols). In **A - D**, $F_z = 15$ N, which, if shown, would be represented by \blacktriangle . The M_z data (Δ) are graphed as $10 \times M_z$. (**A and B**) PDL in the 4 configurations closest to centric and the 4 configurations furthest from centric, respectively. Similarly, (**C and D**) are for the rigid attachment. (**E**) Examples of typical experimental loading protocols

